Absolute Earthquake Locations with Differential Data

By William Menke and David Schaff
Lamont-Dohery Earth Observatory of Columbia University
(corrected version of 6-23-4)

Abstract

Not withstanding the commonly-held wisdom that "you can't determine the absolute location of earthquakes using the double-difference method", you can. We present a way of visualizing double-difference data, and use it to show how differential arrival time data can, in principle, be used to determine the absolute locations of earthquakes. We then analyze the differential form of Geiger's Method, which is the basis of many double-difference earthquake location algorithms, and show that it can be used to make estimates of the absolute location of earthquake sources. Finally, we examine absolute location error in one earthquake location scenario using Monte Carlo simulations that include both measurement error and velocity model error, and show that the double-difference method produces absolute locations with errors that are comparable in magnitude, or even less, than traditional methods. Absolute earthquake locations that are already routinely produced by most implementations of the double-difference method have a better accuracy than has been credited.

Introduction

There has been much recent interest in performing earthquake locations using only relative (differential) arrival times from pairs of earthquakes observed at a common station. This technique, which is often called the *double-difference* method, has two important advantages over traditional earthquake location procedures that use absolute arrival times. First, differential arrival times can be measured very accurately using waveform cross-correlation techniques, and often have variances that are orders of magnitude smaller than the variances of absolute arrival times determined by picking arrivals "by eye". Second, differential traveltimes can be predicted more accurately than absolute traveltimes, because errors in the velocity model tend to cancel out when traveltimes of neighboring events are subtracted [e.g. *Slunga et al., 1995; Waldhauser and Ellsworth, 2000; Wolfe, 2002*]. These advantages allow remarkably high-quality locations. Spatial clusters of earthquakes that, using older methodology, appeared to be only diffuse clouds are now resolved into complex patterns of intersecting fault planes.

There is a prevailing wisdom that the double-difference method also has a major disadvantage, namely that it provides only relative earthquake locations. The method is said to be able to reconstruct the spatial pattern of a cluster of earthquake sources, but not provide information about the overall position of that cluster. An often-heard, rough justification for this idea is that differential traveltimes depend upon the distances between events, so it is those distances that are being reconstructed by the method. The solution process is envisioned as determining a mesh linking the events, with the overall position of the mesh being indeterminate.

This idea is at odds with the results of synthetic tests of the double-difference method [*Waldhauser and Ellsworth, 2000; Menke, 2004*]. In these tests, a set of earthquakes are placed at prescribed positions in an earth model, traveltimes from these events to hypothetical stations are calculated using ray theory and perturbed with random noise, and differential arrival times calculated from the traveltimes and a set of prescribed earthquake origin times. The double-difference method is then used to locate the earthquakes, with the results being compared to the known locations. Typically, the absolute event locations are well-recovered.

Slunga et al. [*1995*] recognized that the justification given above might be misleading. Their implementation of the double-difference method retained the absolute location of the earthquake sources among the unknown variables, because "if the absolute location significantly affects the theoretical arrival time differences" the technique "may improve the absolute location". In this paper, we revisit the question of the sensitivity of differential data to absolute location.

Conceptualizing Differential Arrival Time Data

Consider two earthquake sources, p and q, separated by a small distance, Δs. Let the origin times of these sources be τ_p and τ_q, respectively, the arrival time of the P wave at a receiver at position, $\mathbf{x}$, be $t_p(\mathbf{x})$ and $t_q(\mathbf{x})$, respectively, the traveltime of the P wave from these sources to a receiver at position, $\mathbf{x}$, be $T_p(\mathbf{x})$ and $T_q(\mathbf{x})$, respectively. The differential origin time is defined as $\delta\tau_{pq}=(\tau_p-\tau_q)$, the differential traveltime as $\delta T_{pq}(\mathbf{x})=T_p(\mathbf{x})-T_q(\mathbf{x})$, and the differential arrival time as $\delta t_{pq}(\mathbf{x})= t_p(\mathbf{x})-t_q(\mathbf{x})$.

We first consider the special case of a pair of sources in a box-shaped earth of constant velocity, v. While this case it unrealistic, it serves both to illustrate the general pattern of differential arrival times expected from a pair of sources, and a simple method of using those data to determine the absolute location of the events. Seismic rays in a constant-velocity material are just straight lines, so that the differential traveltime is just (b–a)/v, where b and a are the respective distances from sources p and q to the receiver (Figure 1a). The law of cosines, when applied to triangles pmx and mxq in Figure 1a, implies that $(b^2-a^2)=2r\Delta s\cos(\theta)$, where r is the distance from the midpoint, m, between the two events to the receiver and θ is the angle between this direction and a line connecting the two sources. But algebraically, $(b^2-a^2)=(a+b)(a-b)$, and when r is much larger than Δs, $(a+b)\approx 2r$, so

$$\delta t_{pq}(\mathbf{x}) \approx \delta\tau_{pq} + \Delta s \cos(\theta) / v \qquad (1)$$

This formula is the well-known Fraunhofer approximation. Its application to differential location is discussed in Aki and Richards [*1980*] (Section 14.1.3) and by Fréchet [*1985*], Got et al. [*1994*], and Rubin et al. [*1999*]. At points far from the pair of events, such as on the surface of the box, the pattern of differential arrival times is dipolar (Figure 1b), with an axis of symmetry along the line, R, connecting the two events. The maximum differential time occurs when $\theta=0$ and is approximately $\delta t_{pq}^{max}=\delta\tau_{pq}+\Delta s/v$. The minimum occurs when $\theta=\pi$ and is approximately, $\delta t_{pq}^{min}=\delta\tau_{pq}-\Delta s/v$. The mean differential time, $\delta t_{pq}^{mean}=\delta\tau_{pq}$, occurs on a plane, S, given by $\theta=\pi/2$. This plane is the

locus of all points equidistant from the two sources and the locus of all points of equal traveltime (Figure 1c). There is one point, A, on the surface of the box with the value of δt_{pq}^{max} and there is one point, B, with the value of δt_{pq}^{min}. The mean time occurs along line segments, C, the intersection of S with the box's several faces.

Idealized Earthquake Location Algorithms

Since the differential arrival time on the surface of the box in Figure 1c is a measurable quantity, the positions of points A and B and line C, and the values of δt_{pq}^{max}, δt_{pq}^{min}, δt_{pq}^{mean} can, in principle, be determined by observation. The event separation can then be calculated as $\Delta s = v(\delta t_{pq}^{max} - \delta t_{pq}^{min})/2$, and the differential origin time can be calculated as $\delta\tau_{pq} = \delta t_{pq}^{mean}$. Furthermore, the midpoint between the events can be determined. It is on the line, R, connecting A and B, at the point where a plane perpendicular to R intersects C. The events are located on the line, distances of $\pm\Delta s/2$ from the midpoint. It is therefore clear that measurements of the differential arrival time for two events are sufficient to determine their absolute locations. Note that we have assumed here that the velocity, v, is a known quantity (that is, it has been precisely determined by independent means such as a seismic refraction experiment). We discuss the impact of the practical problem of velocity model error later in the paper.

Knowledge of the position of the symmetry axis, alone, is sufficient to allow events to be located, provided that differential arrival time data for several overlapping pairs of events are available. Suppose that we know the position of points A and B for a pair (p,q) of events (let's call these points, A_{pq} and B_{pq}). Events p and q must lie on the line connecting A_{pq} and B_{pq} (Figure 1d). Suppose that we also know the position of points A_{pr} and B_{pr} for the (p,r) pair of events. Events p and r must lie on the line connecting these two points. Event p must therefore lie at the intersection of the two lines. Similarly, the other two events, q and r, must lie at the intersection of analogous lines. The absolute position of the events can be determined solely through knowledge of where on the surface of the box the differential arrival time is minimum and maximum. It is therefore clear that having information about overlapping pairs of events helps with the location process

Now let us consider the more realistic case of a vertically-stratified velocity structure (that is, $v(\mathbf{x})=v(z)$, where z is depth). Like the constant velocity case, the pattern of differential arrival times also possesses symmetry, in this case mirror symmetry about the vertical plane that contains the two sources (Figure 2a). Once again, the measurements of the line of symmetry on the surface of the earth can be used to constrain the location of the events: Since events p and q must lie on the vertical plane beneath the line of symmetry of δt_{pq}, and events p and r must lie on the vertical plane beneath the line of symmetry of δt_{pr}, event p must lie on the vertical line defined by the intersection of the two planes. Only the horizontal coordinates, (x,y), and not the depth, z, of the event are determined.

To proceed further, we must make some assumptions about the way in which the velocity field varies in the vicinity of the events. If it possesses strong variability over length scales smaller than the event separation, then the pattern of differential arrival times might be very complicated, or even ill-defined (if, for example, one event was shadowed from a given receiver, while the other wasn't). We will restrict ourselves to

cases where it varies sufficiently slowly that ray paths are simply "curvy" versions of the straight lines of the constant-velocity case. Far from a pair of events, we would then expect that the differential arrival time would be – at least approximately – a generalized version of Equation 1:

$$\delta t_{pq}(\mathbf{x}) \approx \delta\tau_{pq} + \Delta T \cos(\theta) \tag{2}$$

Here ΔT, the traveltime from the location of event p to q, is a generalization of the quantity, $\Delta s/v$, in Equation 1. It is computed along the ray, R, connecting the two events (Figure 3). The angle, θ, is now understood to mean the takeoff angle of a ray from the midpoint between the sources to the receiver at position, **x**, measured with respect to the line connecting the sources. A key property of this formula is that the minimum and maximum differential arrival times occur along R.

When this approximation holds, then differential arrival times are just the dipolar function from the constant-velocity case, projected along rays that diverge from the source midpoint onto the surface of the earth (Figure 4). In the vertically-stratified case, several special cases are worth examining: When events p and q are separated by a purely horizontal distance increment, then the points A and B are in the vertical plane containing the sources, and line C is the perpendicular bisector of line AB (Figure 5a); When the events are separated by a purely vertical distance increment, then the point A is directly above the events and the curve, C, is a circle centered on A (Figure 5b). More generally (and not limited to the vertically-stratified case), the location algorithms from the constant-velocity case have simple generalizations: Once the points A and B are known, the ray, R, can be found by raytracing from A to B. The midpoint between the events is the point on R from which a suite of rays, when raytraced from this point perpendicular to R, intersect C. As in the constant-velocity case, when data from several overlapping pairs of events are available, the events can be located by finding points of intersection between rays (Figure 5c).

The patterns in Figures 4, 5a, and 5b can be observed in actual data. Figure 6 shows four pairs of earthquakes on the San Andreas Fault at Parkfield recorded on the short-period, vertical component Northern California Seismic Network (NCSN). Shaded contours show the theoretical distribution of differential arrival times, calculated by raytracing through an appropriate vertically-stratified earth model. Individual boxes indicate the observed arrival times for each station, which in general are in very good agreement with the underlying theoretical distribution. In Figures 6a and 6b, the pattern of the differential arrival times corresponds closely to the expected horizontal separation pattern in Figures 4a & 5a. The pairs are both separated by 310 m leading to δt_{pq}^{max} of about 0.06 s. These measurements are made by waveform cross correlation which have precision below the sample level (0.01 s) — sufficient to reveal the pattern in differential arrival times for these separation distances. For longer separation distances and larger events, ordinary phase pick data can produce the expected patterns over a broad scale as well (Figures 6c & 6d). The event pair in Figure 6c is separated by 4.5 km, mostly in the vertical, and therefore matches best with the patterns in Figures 4b & 5b. The event pair in Figure 6d has a separation of 5.6 km and has the expected theoretical pattern for an inclined separation vector (Figure 4c).

The accuracy of the approximation in Equation 2 is difficult to assess in general. We give here an analysis of one specific case, that of events separated by a purely horizontal distance increment in a vertically-stratified medium (Figure 7a). This configuration is one where we might expect the accuracy of the approximation to be poorest, since the velocity gradient is perpendicular to the line connecting the sources, and a ray propagating from one source towards the other will have maximum curvature.

Let the traveltime from a source at position, $(x,z)=(0,z_0)$ to a receiver at position $(x,z)=(0,x)$ be $T(x)$. In many relevant earth models, where $v(z)$ monotonically increases with depth, this function will resemble the sketch in Figure 7b. The traveltime increases with range, x, and passes through an inflection point at some range, x_0, that corresponds to a ray that leaves the source exactly horizontally. The horizontal slowness, dT/dx, reaches a maximum of $1/v(z_0)$ at this range (Figure 7c).

Suppose that sources p and q are located at depth, z_0, with horizontal positions $-h$ and h, respectively. The differential traveltime at position, x, is $\delta T_{pq}(x) = T(x+h) - T(x-h)$. We now expand this formula in a Taylor series:

$$\delta T_{pq}(x) = 2h\, dT/dx + O(h^3) \tag{3}$$

To a high degree of accuracy (that is, to order h^2), the differential traveltime is maximum when the slowness, dT/dx, is maximum. But dT/dx has a maximum value at the point, x_0. As predicted by Equation 2, the maximum differential traveltime occurs along a ray that leaves the source midpoint traveling exactly horizontally (for a horizontal separation). The slowness of the ray associated with event p is dT/dx measured at the point, $x=x_0+h$, and the slowness of the ray associated with event q is dT/dx measured at the point, $x=x_0-h$. Since dT/dx has a maximum of $1/v(z_0)$ at x_0, these two slownesses at points to either side of this maximum are approximately equal, with a value somewhat less than $1/v(z_0)$. The degree of deviation from equality will depend upon the asymmetry of the peak in dT/dx, that is, upon the magnitude of d^3T/dx^3, but will always be negligible for sufficiently small h. The fact that the rays leaving sources p and q have the same horizontal slowness implies that they are the same ray. The approximation of Equation 2 is valid in this case.

We have also tested the approximation numerically, for a variety of non-horizontal source locations, in a vertically-stratified earth model with a velocity gradient of 0.08 s^{-1}. It performed well in all cases.

The discussion so far has been directed towards understanding the pattern of differential arrival times associated with two neighboring sources, and in demonstrating that these patterns contain information about the absolute location of those sources. The location algorithms are presented to help make the case that the differential data are sufficient to provide absolute locations. They are "thought experiments", only. No claim is being made that they should supplant well-established location procedures, or indeed, that they are of any practical use, whatsoever. Indeed, our experience is that existing implementations of the double-difference method that are based on generalizations of Geiger's Method work well.

The Differential Form of Geiger's Method Can Estimate Absolute Locations

Let us first examine the process of forming differential data. Suppose that we have N absolute data, $\{d_i, i=1, \ldots N\}$. We can form N linear combinations of these data:

$$\begin{gathered}\text{the sum, } \Sigma_{i=1}^{N} d_i \\ \text{and} \\ (N-1) \text{ differences } \{\delta d_{12}, \delta d_{23}, \delta d_{34}, \ldots \delta d_{N(N-1)}\}, \text{ (with } \delta d_{pq}=d_p-d_q)\end{gathered} \tag{4a}$$

These N linear combinations are complete, in the sense that the original data can be computed from them:

$$\begin{gathered}N d_1 = \Sigma_{i=1}^{N} d_i + (N-1)\,\delta d_{12} + (N-2)\,\delta d_{23} + \ldots + (1)\,\delta d_{(N-1)N} \\ d_2 = d_1 - \delta d_{12} \\ d_3 = d_2 - \delta d_{23} \\ \ldots \\ d_N = d_{(N-1)} - \delta d_{(N-1)N}\end{gathered} \tag{4b}$$

Note that this strategy for representing differential data is not the same as the one used by *Wolfe [2002]*, in which each datum, d_i, is represented by its deviation, Δd_i, from the mean position (that is, $d_i = (1/N)\Sigma_{j=1}^{N} d_j + \Delta d_i$). While intuitively appealing, Wolfe's approach has the drawback of creating (N+1) linear combinations of data (the mean position and N deviations), rather than precisely N of them. Note that in Equation 4a, considerable latitude is available for choosing which set of (N−1) differences to use, since $\delta d_{pq}=-\delta d_{qp}$, and $\delta d_{pq}=\delta d_{pr}-\delta d_{qr}$. The only requirement for the representation being complete is that the indice of each of the N events appear at least once in the set of N−1 differences, $\{\delta d_{ij}\}$. Finally, note that if a complete set of (N−1) differential data are available, we are missing only one piece of information needed to reconstruct the N absolute data − the sum, $\Sigma_{i=1}^{N} d_i$.

In analyzing Geiger's Method, we first note that it is based on the arrival time equation:

$$t_{pk} = \tau_p + T_{pk}, \tag{5}$$

for source, p, and receiver, k, where T represents traveltime. (Here we assume that there are N sources and M receivers). The method starts by linearizing this equation about a trial source location, $\mathbf{x}^0_p$, and keeping only the first order terms:

$$\tau_p + \nabla T_{pk} \cdot \Delta \mathbf{x}_p = t_{pk} - T^0_{pk} \tag{6}$$

Here the gradient is taken with respect to the source coordinates and evaluated at the trial location. The quantity, T^0_{pk}, is the traveltime evaluated at the trial location. The solution to Equation 5 provides an estimate of a correction, $\Delta \mathbf{x}_p$, to the trial location. A key

element of Geiger's Method is the recognition that the gradient of the traveltime is just the slowness, $\mathbf{u}$, of the ray as it leaves the source, so that $\nabla T_{pk} = \mathbf{u}_{pk}$. (By slowness, we mean a vector parallel to the ray with magnitude of the reciprocal of the local velocity). Equation 6 can be iterated, to provide a succession of ever-improved locations.

Geiger's Method can be adapted to differential data simply by recasting Equation 5 from its "absolute" to "differential" representation

$$\Sigma_{p=1}^{N}\tau_p + \Sigma_{p=1}^{N} T_{pk} = \Sigma_{p=1}^{N} t_{pk} \tag{7a}$$

$$\delta\tau_{pq} + [T_{pk} - T_{qk}] = \delta t_{pqk} \tag{7b}$$

Equation 7a is not available when the data are limited to differential arrival times. It is apparent that Equation 7b is insufficient to determine absolute origin time, since it contains only the differences, $\delta\tau_{pq}$, and not the sum, $\Sigma_{p=1}^{N}\tau_p$. However, the more important question is the degree to which Equation 7b can be used to determine absolute positions. We address this question by transforming from absolute positions, $\{\mathbf{x}_p, p=1, \ldots, N\}$, to their sum and differences. In order to keep variable names of manageable length, we will denote the sum, $\Sigma_{p=1}^{N}\mathbf{x}_p$, and the differences, $\delta\mathbf{x}_{p,p+1}=\mathbf{x}_p-\mathbf{x}_{p+1}$, with the symbols, $\boldsymbol{\sigma}$ and ξ_p, respectively.

We now view the traveltime as a function of the N transformed variables: $T_{pk}(\boldsymbol{\sigma},\xi_1,\xi_2,\ldots,\xi_{N-1})$, and linearize it about the trial locations, $(\boldsymbol{\sigma}^0,\xi^0_1,\xi^0_2,\ldots,\xi^0_{N-1})$:

$$T_{pk}(\boldsymbol{\sigma},\xi_1,\xi_2,\ldots,\xi_{N-1}) = T^0_{pk} + \partial T_{pk}/\partial\boldsymbol{\sigma} \cdot \Delta\boldsymbol{\sigma} + \Sigma_{m=1}^{N-1}\partial T_{pk}/\partial\xi_m \cdot \Delta\xi_m \tag{8}$$

We expect, as before, that the partial derivatives are related to the slowness vector. We uncover this relationship by using the chain rule:

$$\partial T_{pk}/\partial\boldsymbol{\sigma} = \Sigma_{n=1}^{N} [\partial T_{pk}/\partial\mathbf{x}_n] [\partial\mathbf{x}_n/\partial\boldsymbol{\sigma}] \quad \text{and} \quad \partial T_{pk}/\partial\xi_m = \Sigma_{n=1}^{N} [\partial T_{pk}/\partial\mathbf{x}_n] [\partial\mathbf{x}_n/\partial\xi_m] \tag{9}$$

As indicated above, the gradient of the traveltime from event, p, at station, k, is $\mathbf{u}_{pk}$. Since the traveltime from event, p, depends only upon the location of event, p, we have $\partial T_{pk}/\partial\mathbf{x}_n = \mathbf{u}_{pk}\,\delta_{pn}$, where δ_{pn} is the Kronecker delta. The other two derivatives can be found by substituting the event locations and transformed variables into Equation 4 and then differentiating:

$$\begin{aligned}
x_1 &= \boldsymbol{\sigma}/N + [(N-1)/N]\,\xi_1 + [(N-2)/N]\,\xi_2 + \ldots + [1/N]\,\xi_{N-1} \\
x_2 &= \boldsymbol{\sigma}/N + [(N-1)/N - 1]\,\xi_1 + [(N-2)/N]\,\xi_2 + \ldots + [1/N]\,\xi_{N-1} \\
&\ldots \\
x_N &= \boldsymbol{\sigma}/N + [(N-1)/N - 1]\,\xi_1 + [(N-2)/N - 1]\,\xi_2 + \ldots + [1/N - 1]\,\xi_{N-1}
\end{aligned} \tag{10a}$$

Since Equation 10a consists of linear functions with constant coefficients, it is apparent that its derivatives will be simple numbers. We find that $\partial\mathbf{x}_n/\partial\boldsymbol{\sigma} = 1/N$ and

$$\partial \mathbf{x}_n / \partial \boldsymbol{\xi}_m = A_{nm} \quad \text{where } A_{nm}=(N-m)/N \text{ if } m \geq n \text{ and } A_{nm}=-m/N \text{ if } m<n \tag{10b}$$

The derivatives in Equation 9 are then $\partial T_{pk}/\partial \boldsymbol{\sigma} = \mathbf{u}_{pk}/N$ and $\partial T_{pk}/\partial \boldsymbol{\xi}_m = A_{pm}\mathbf{u}_{pk}$. The linearized form of Equation 7b is:

$$\delta\tau_{pq} + (\mathbf{u}_{pk}-\mathbf{u}_{qk}) \cdot \Delta\boldsymbol{\sigma}/N + \Sigma_{m=1}^{N-1} [A_{pm}\mathbf{u}_{pk}-A_{qm}\mathbf{u}_{qk}] \cdot \Delta\boldsymbol{\xi}_m = \delta t_{pqk} - \delta T^0_{pqk} \tag{11}$$

This equation is the basic algorithm of the double-difference method, or at least those versions of it that are generalizations of Geiger's Method. Here we have used the abbreviation, $\delta T^0_{pqk}=T^0_{pk}-T^0_{qk}$, for the differential traveltime evaluated at the trial location. Note that Equation 11 contains both $\Delta\boldsymbol{\sigma}$ and $\Delta\boldsymbol{\xi}_m$, that is, it contains information about both the absolute and relative locations of the events. However, when the events are close to one another, the slownesses of rays from these sources to a common receiver will be similar. Thus, the quantity, $(\mathbf{u}_{pk}-\mathbf{u}_{qk})$, in Equation 11, which multiplies the "mean location correction", $\Delta\boldsymbol{\sigma}/N$, will typically be smaller in magnitude than the quantity, $[A_{pm}\mathbf{u}_{pk}-A_{qm}\mathbf{u}_{qk}]$, which multiplies the "differential location corrections", $\Delta\boldsymbol{\xi}_m$.

Wolfe [2002] notes both relative locations and the hypocentroid can potentially be resolved with the double-difference method, but that if the earthquakes are confined to a small spatial region such that the partial derivatives are only slightly different, the inversion may be unstable with real data, due to three small singular values for the hypocentroid position. In order to analyze the impact of this difference in size of the above corrections, we consider the special case of N=2, that is, locating just a single pair of events. Equation 11 simplifies to:

$$\delta\tau_{12} + (\mathbf{u}_{1k}-\mathbf{u}_{2k}) \cdot \Delta\boldsymbol{\sigma}/2 + \tfrac{1}{2}(\mathbf{u}_{1k}+\mathbf{u}_{2k}) \cdot \Delta\boldsymbol{\xi}_1 = \delta t_{12k} - \delta T^0_{12k} \tag{12}$$

Now suppose that the earth has constant velocity, v, and that the receiver is at distance, r, from the source midpoint. The slowness vectors can be computed analytically, with the result that $|(\mathbf{u}_{1k}-\mathbf{u}_{2k})| \propto \Delta s/(rv)$ and $|(\mathbf{u}_{1k}+\mathbf{u}_{2k})| \propto 1/v$. The coefficients of $\Delta\boldsymbol{\sigma}$ and $\Delta\boldsymbol{\xi}_1$ in Equation 12 differ by a factor of $\Delta s/r$, that is, the ratio of the source separation to the source-receiver range. In a regional earthquake location scenario, Δs would be of the order of 10–1000 m, while r would be of the order 10^4–10^5 m, so the ratio would be of order 10^{-4}–10^{-1}. While smaller than unity, these are by no means negligibly small values. Ratios of this size are encountered in many other perfectly tractable problems, such as the least-squares fitting of polynomials. Furthermore, in realistic problems there will not be just two events with a single separation, Δs, but many events with a ensemble of inter-event separations. The ability of the double-difference method to estimate the absolute position of the events will be controlled by the largest Δs's for which differential traveltimes can be reliably estimated. The double-difference method (as embodied in Equations 11 and 12) has at least some ability to estimate the absolute position of the events.

A Numerical Simulation to Test Sensitivity to Measurement Error

We compute estimates of the variance of location errors arising from measurement error using a Monte-Carlo simulation. Fifty sources are placed in vertically-stratified earth model, arranged in a 5×10 grid on a vertical plane, with depths varying between 3 and 6 km (Figure 8). The spacing between the sources is prescribed to be 1 km horizontally and 0.33 km vertically. We compute exact ray-theoretical traveltimes between these sources and 9 receivers arranged in an X-shaped array, using a simple, vertically-stratified earth model and Menke's [*2004*] RAYTRACE3D software. We then use these traveltimes, together with prescribed origin times, to produce 450 absolute arrival times and 11025 differential arrival times. We then add random noise to these data, locate the sources by both the traditional method and the double-difference method, and examine the statistics of the location errors.

The RAYTRACE3D software calculates raypaths and traveltimes in a three-dimensionally heterogeneous earth and implements both traditional and double-difference earthquake location methods. The linearized version of Geiger's Method, for both absolute and differential traveltimes (that is, Equations 5 and 7) are constructed using partial derivatives based on 3D raytracing and solved with a damped-least squares process that employs a biconjugate gradient matrix solver.

Suppose that a receiver records each of the N=50 sources. One question that arises is whether to use all N(N−1)/2=1225 possible differential traveltimes when locating the sources with the double-difference method. Inclusion would be clearly inappropriate if we were simulating the case in which the differential arrival times were computed from the absolute arrival times by simple subtraction. The errors of the 1225 differential data are not independent, but rather are highly correlated. Thus, if $\delta t_{12}=t_1-t_2$ and $\delta t_{13}=t_1-t_3$ and if the t_i have uncorrelated random error with variance σ^2, then δt_{12} and δt_{13} will both have a variance of $2\sigma^2$, and a non-zero covariance of σ^2. Even though one appears to have increased the number of data from 50 to 1225 by going from absolute to differential data, the number of degrees of freedom of the differential data is in fact 49. But in reality, the differential arrival times are computed by cross-correlation, using seismograms that contain some large number, say L, of discrete samples. The number of degrees of freedom of the seismogram data might therefore be as high as M×L (depending upon the bandwidth of the noise), and in any case may be much larger than N. The degree of correlation of differential arrival times made by cross-correlation may be less than in the arithmetic case discussed above (which has an expected correlation coefficient of 0.5).

We are unaware of any theoretical treatment of this issue. We show here a numerical test (Figure 9), in which the correlation is much less in the cross-correlation case than the arithmetic case (correlation coefficients of 0.2 and 0.5, respectively). We feel that this low correlation justifies our inclusion of all differential arrival time data in the simulation.

We add uncorrelated, normally-distributed random noise (standard deviation, 0.01s) to both the absolute and differential arrival time data. We also perturb both the starting parameters of the events in the following way: we add uncorrelated, normally-distributed random noise to the origin time and x, y and z coordinates of each event individually (standard deviation, 0.5 km and 0.5 s, respectively). We then add uncorrelated, normally-distributed random noise to the mean origin time and x, y and z

components of the mean position (standard deviation, 0.5 km and 0,5 s, respectively). This two-step process ensures that both the absolute and relative starting positions of the events are far off their true values. The simulation is repeated fifty times, the events are located for both the traditional method and the double-difference method and their errors statistics are calculated (Figure 10). The absolute location errors of the double-difference method have a standard deviation of about 10 meters, while the standard deviation of the traditional method is more than three times that value, about 35 meters. The difference is entirely due to the larger amount of data associated with the double-difference method ($N(N-1)/2$ per station, compared with N in the traditional method), plus the assumption that the noise in these data is uncorrelated. The larger amount of data results in more noise cancellation during the solution process. As discussed above, the assumption that differential traveltime data are uncorrelated (or poorly-correlated) is plausible, but by no means proven.

We examine the alternative case of highly-correlated data by repeating the simulation (not shown), but using only $N-1$ (as contrasted to $N(N-1)/2$) differential arrival times from each station. There are many ways to choose which set of $N-1$ pairs to use, requiring only that all N events are represented. We randomly choose a different set for each station, since using a single set implies an artificial ordering of the events, and leads to bias. In this case, the absolute location errors of the double-difference method have a standard deviation of about 70 meters, and are clearly worse than those from the tradition method. On the other hand, this simulation uses the same standard deviation (0.01 second) for the error in both absolute and differential arrival time data. When cross correlation is used, the error of differential arrival times may be much smaller. We repeat the simulation, now with a standard deviation of 0.001 second for the error in the differential data, and the error in double-difference absolute locations drops to 7 meters. Using this more realistic error scenario, the double-difference method has the smaller error in absolute locations.

A Numerical Simulation to Test Sensitivity to Velocity Model Error

One of the claims made of the double-difference technique is that is it is relatively insensitive to errors in the velocity model, and in particular, to unmodeled near-station heterogeneities. The idea is that the traveltimes of rays from neighboring events to a common station are affected almost equally by the heterogeneity near that station, so that near-perfect error cancellation occurs when those traveltimes are differenced. Whether the double-difference technique is insensitive to other types of velocity model errors is less clear, and indeed may depend upon the location and scale length of the particular unmodeled velocity heterogeneities under consideration. We present a series of numerical simulations, similar to the ones presented above, that test sensitivity to velocity model error. We use the same source and receiver geometry as is shown in Figure 8, but we now perturb the vertically-stratified velocity structure shown in Figure 8 with random heterogeneities prior to computing absolute and differential traveltimes. We use additive heterogeneities of the form:

$$\Delta v \exp\{ (x-x_0)^2/s_x^2 + (y-y_0)^2/s_y^2 + (z-z_0)^2/s_z^2 \} \tag{13}$$

This is a Gaussian heterogeneity centered at (x_0, y_0, z_0) and with scale lengths of s_x, s_y, s_z in the x, y, and z directions, respectively. The overall amplitude, Δv, is randomly chosen from a normal distribution with zero mean and a variance, σ^2_v.

We examine the effect of near-station velocity model error by placing one of these heterogeneities beneath each station, with z_0=0, (s_x, s_y, s_z) = (5, 5, 2 km), and three different intensities of heterogeneity, σ_v = 0.01, 0.10 and 1.00 km/s. We compute exact (and noise-free) ray-theoretical absolute and differential traveltimes through this three-dimensional model, and then locate the earthquakes in an erroneous model (the vertically-stratified one). Fifty realizations are computed for each choice of σ_v, and statistics for errors in both absolute and differential locations are calculated. The results indicate that the double-difference method (solid curves in Figure 11) produces both absolute and differential locations that have significantly less error, by a factor of 1.5–4, than traditional locations based on absolute traveltimes (bold curves in Figure 11). In all cases, the error in the relative location is less than the error in the absolute location determined using the same location technique. But the use of differential traveltime data, which are insensitive to near-station heterogeneity, leads to an improvement in *both* absolute and differential locations (meaning the nearest-neighbor distances). Even with the rather enormous model error of σ_v = 1 km/s, the standard deviation of the absolute location, as determined by the double-difference method, is only 155 m (horizontally), or 15% of the event spacing. This would in our opinion constitute a usefully accurate absolute location in many applications. The standard deviation of the corresponding relative location is astoundingly small, only 25 m (horizontally), or 2.5% of the event spacing, thus reinforcing the notion that the double-difference technique does exceptionally well in determining differential locations.

We have also examined the effect of volumetric velocity model error (Figure 12) and near-source velocity model error (Figure 13) on location accuracy. As in the near-station case, the error in the relative location is less than the error in the absolute location determined using the same location technique by a factor of 2-4. But the errors for the double-difference locations are not systematically better (or worse) than those of the traditional method.

The volumetric case that we examine has an earth model with ten heterogeneities, each with the horizontal scale lengths of (s_x, s_y) = (10, 10 km) that are comparable to typical source-station offsets. This case might be considered a worst-case scenario, since a ray will typically have most of its path length in a single heterogeneity and consequently accumulate a large perturbation in traveltime. In this case, the absolute locations, as determined by the double-difference method, have a standard deviation of 100 m (or 10% of the inter-event spacing; what we could still consider usefully accurate) at a degree of heterogeneity of σ_v = 0.2 km/s (or 5–10% of the laterally-averaged velocity). The corresponding root-mean-square error in absolute traveltime is 0.1 s. There will, of course, be causes where one wants to locate earthquakes in places where almost no information on the earth model is available, and where velocity model errors may well exceed the 5-10% figure cited above. Absolute earthquake locations in such regions may well be completely unreliable. Nevertheless, our sense is that the 5-10% standard is not a hard one to achieve, especially in areas where geologic, seismic refraction, well-log, etc. data can be used to constrain the velocity structure. Furthermore,

to the extent that the effect of the unmodeled velocity structure can be detected in the differential traveltime data, joint inversion techniques that estimate both 3D velocity variations and earthquake locations can be employed [*Zhang and Thurber, 2003*].

Conclusions

One might be tempted to say that earthquake locations are "good" or "poor". But such judgments are necessarily relative. We must ask, better or poorer compared to what other estimate, or good enough or too poor for what specific purpose?

Suppose we were to make direct measurements of absolute arrival time, t_{pk}, (say by phase-picking) and then calculate the sum, $\Sigma_{p=1}^{N} t_{pk}$, and the differences, δt_{pqk}. The estimate of the absolute location of the events, based on the double-difference method (Equation 11), will certainly be poorer than if the events were located individually via traditional methods (Equation 6). The estimate obtained without the use of a critical piece of information – the sum, $\Sigma_{p=1}^{N} t_{pk}$ – results in a poorer estimate than when that information is used. But this scenario ignores the reality that differential arrival times can be measured directly by cross-correlation, and that their variances are typically much smaller than the variance of absolute arrival times determined by phase-picking. Absolute locations determined using high-precision differential times might well have smaller variances than those determined with low-precision phase-picked absolute times. In this case, the absolute locations produced by the double-difference method are better than those produced by traditional methods.

Because the underlying equation (Equation 11) of the double-difference method is relatively insensitive to the mean location, the variance of the absolute locations will typically be larger than the variance of the inter-event distances. Thus, it is fair to say that the absolute locations are poorer than the relative locations, when both are obtained using the double-difference method. But that does not necessarily imply that the absolute locations are useless, since that judgment must be made on the basis of the actual magnitude of their variance. The absolute locations may well be good enough to permit them to be used in some specific application.

While it might seem logical to think that absolute locations are best determined by using absolute traveltime data, this idea does not appear to be true. Absolute locations determined using differential data are typically as good as, and sometimes much better than, absolute locations determined using traditional techniques. The improvement is particularly striking in the case of unmodeled near-station heterogeneity.

Reliance on differential traveltimes determined by cross-correlation produces an interesting paradox: The accuracy of absolute locations increases with increasing source separation. But due to the distortion of seismic waveforms by scattering, the accuracy of cross-correlation data decreases with source separation. So, widely-separated sources have both a "good" and a "bad" effect on the location process. Fortunately, in actual cases (e.g. Figure 6), cross-correlation work well out to source separations of a few hundred meters to a few kilometers, and is adequate for determining absolute locations accurate to with tens to hundreds of meters (at least in our simulations).

The variance of the absolute positions will depend upon the original variance (and covariance) of the differential traveltime data, to the variance of velocity model error and the degree to which variance reduction occurs through the process of combining

observations from many receivers during the solution of Equation 11. The variance of the data, the variance of the velocity model and the geometry of the observations – which strongly affects the structure of Equation 11 – differ widely between experiments. Absolute locations (along with their variances) should be estimated routinely, and their usefulness assessed on a case-by-case basis.

In conclusion, we urge that more attention be given to absolute earthquake locations that are already routinely produced by most implementations of the double-difference method. Their accuracy is better than has been credited.

Acknowledgements. We thank Felix Waldhauser and Paul Richards for helpful discussion. This research was supported by the National Science Foundation under grant OCE 02-21035. Lamont-Doherty Contribution Number 0000.

References

Aki, K, and P. Richards, Quantitative Seismology: Theory and Methods, W.H. Freeman and Company, San Francisco, 1990.

Fréchet, J., Sismogenèse et doublets sismiques, Thèse d'Etat, Université Scientifique et Médicale de Grenoble, 206 pp., 1985.

Got J.-L., J. Fréchet, and F. W. Klein, Deep fault plane geometry inferred from multiplet relative relocation beneath the south flank of Kilauea, *J. Geophys. Res*., *99*, 15,375-15,386, 1994.

Menke, W., Case studies of seismic tomography and earthquake location in a regional context, in *Seismic Data Analysis and Imaging With Global and Local Arrays*, Alan Levander and Guust Nolet, Eds., American Geophysical Union, in press 2004.

Rubin, A.M., Gillard, and J.-L. Got, Streaks of microearthquakes along creeping faults, *Nature, 400*, 635-641, 1999.

Slunga, R., S.T. Rognvaldsson and B. Bodvarsson, Absolute and relative locations of similar events with application to microearthquakes in southern Iceland, *Geophys. J. Int. 123,* 409-419, 1995.

Waldhauser, F. and W. Ellsworth, A double-difference earthquake location algorithm; method and application to the northern Hayward Fault, California*, Bull. Seis. Soc. of Am.. 90*, 1353-1368., 2000.

Wolfe, C. J., On the mathematics of using difference operators to relocate earthquakes, , *Bull. Seis. Soc. of Am., 92*, 2879-2892, 2002.

Zhang, H. and C.H. Thurber, Double-Difference Tomography: The Method and Its Application to the Hayward Fault, California, *Bull. Seis. Soc. of Am., 93,* 1875-1889, 2003.

Figure Captions

Figure 1. Differential arrival times in a constant-velocity earth model. A) Geometery used to calculate the differential traveltime from sources p and q to a receiver at **x**. B) The differential arrival time varies as the cos(θ). C) The differential traveltime has maximum and minimum along line R, and mean value along plane, S. Line R intersects the surface of the earth model at points A and B. Plane S intersects the surface of the model along line, C. D) Location algorithm that uses two overlapping pairs of events, (p,q) and (p,r) to locate event, p.

Figure 2. A) Differential arrival times in a vertically-stratified earth model are symmetric about the vertical plane containing the sources. B) Location algorithm that uses two overlapping pairs of events, (p,q) and (p,r) to determine the horizontal coordinates of event, p.

Figure 3). Definition of the qualities R and θ in A) a constant-velocity earth model, and B) a heterogeneous earth model with smoothly varying velocity.

Figure 4). Differential traveltimes on the surface of a vertically-stratified earth model. The two sources separated by 141 meters. The six cases differ in source depth (A, B, C, depth=3100 meters; D, E, F, 2100 meters) and orientation (A, D, horizontal; B, E, vertical; C, F, 45° dip). The contour level is 0.002 second. The mean differential traveltime contour is shown in bold. The earth model has monotonically-increasing velocity, with velocities of (3.0, 3.5, 4.0, 5.0, 6.0, 7.0, 7.7) km/s at depths (0, 1000, 2000, 5000, 8000, 13000, 18000) meters. The differential arrival times were calculated by ray tracing using Menke's [2004] RAYTRACE3D software.

Figure 5. Differential traveltimes in a vertically-stratified earth model. A) When the line connecting sources p and q is horizontal, points A and B are in the vertical plane containing the sources, and that line C is the perpendicular bisector of the line AB. B) When the line connecting sources p and q is vertical, the point A is directly above the sources and the curve C is a circle centered on A. C). Location algorithm that uses two overlapping pairs of events, (p,q) and (r,q) to determine the location (including the depth) of event, q.

Figure 6. Comparison of observed (boxes) and theoretical differential traveltimes (shaded contour maps) for four pairs of events on the San Andreas Fault at Parkfield. Midpoint of each pair is located at the origin. Bold black line indicates zero mean level. A) & B) measurements are from waveform cross correlation data with coefficients > 0.8. C) & D) are derived from high quality P-wave picks (weights 0 & 1). Separation distances are 310 m, 309 m, 4.5 km, and 5.6 km, respectively. Number of stations observing are 45, 52, 87, and 93, respectively.

Figure 7. Analysis of differential traveltimes from horizontally-separated sources in a vertically-stratified earth model. A) A ray that leaves the source midpoint $(0,z_0)$ horizontally touches the earth's surface at point $(0,x_0)$. A ray that passes through sources p and q also touches this point. B) Traveltime of a source at $(0,z_0)$ to an observer at (0,x). Note that the curve has an inflection at x_0. C) Corresponding horizontal slowness, dT/dx, reaches a peak value at x_0. Note that the horizontal slownesses of two points offset from x_0 by $\pm h$ are approximately equal.

Figure 8. Geometry of earthquake location simulation. Nine receivers are arranged on the surface of the earth model in an X-shaped array. Fifty sources are arranged in a 5×10 grid on a vertical plane between depths of 3 and 6 km. The velocity structure is vertically stratified.

Figure 9. Statistics of differential traveltimes. A) Three seismograms, constructed by adding band-limited random noise to a deterministic P wave pulse. Differential times, δt_{12} and δt_{13} are calculated from these seismograms using cross-correlation. B) Scattergram of δt_{12} and δt_{13} for 1000 realization of the set of three seismograms. Each dot on the plot corresponds to one pair of δt_{12} and δt_{13} computed by cross-correlating two pairs of seismograms. These data have a correlation coefficient of r=0.22. C) Comparison scattergram computed by subtracting arrival times has correlation coefficient r=0.53 (0.5 expected theoretically).

Figure 10. Location errors from the simulation in Figure 8, quantified using histograms. The results are based on 50 realizations, with the location errors of all earthquakes being lumped together. Initial source locations are the exact locations perturbed by adding normally-distributed random numbers with 0.5 km standard deviation to the mean event location, and to the location of each source, individually. Bold: the traditional method, using absolute arrival time data computed from exact arrival times plus 0.01s random error. Solid: double-difference method, using differential arrival times computed from the exact differential data plus 0.01s random error. Note that the double-difference method tends to have smaller location errors.

Figure 11. Location errors due to unmodeled near-station velocity model heterogeneity, quantified using histograms. Histograms are computed in a manner analogous to that of Figure 10. The vertically-stratified earth model is perturbed with 9 heterogeneities (one beneath each station) with $z_0=0$, $(s_x, s_y, s_z) = (5, 5, 2$ km), and three different intensities of heterogeneity, $\sigma_v = 0.01$, 0.10 and 1.00 km/s Bold: the traditional method, using absolute arrival time. Solid: double-difference method. The standard deviations in locations, σ_x, are listed for the traditional first and the double-difference second in each subplot. The root-mean-square absolute traveltime error, ΔT, corresponding to each level of heterogeneity, σ_v, is given. Standard deviations, σ_x, of the traditional and double-difference estimates of horizontal position (in that order) are given for each plot. The double-difference method tends to have *both* smaller absolute and smaller relative location errors.

Figure 12. Location errors due to unmodeled volumetric velocity model heterogeneity, quantified using histograms. Histograms are computed in a manner analogous to that of Figure 10. The vertically-stratified earth model is perturbed with 10 heterogeneities with (x_0, y_0, z_0) chosen randomly, $(s_x, s_y, s_z) = (10, 10, 3$ km), and three different intensities of heterogeneity, $\sigma_v = 0.01$, 0.10 and 1.00 km/s. Bold: the traditional method, using absolute arrival time. Solid: double-difference method. The root-mean-square absolute traveltime error, ΔT, corresponding to each level of heterogeneity, σ_v, is given. Standard deviations, σ_x, of the traditional and double-difference estimates of horizontal position (in that order) are given for each plot. The traditional and double-difference methods yield similar errors.

Figure 13. Location errors due to unmodeled near-source velocity model heterogeneity, quantified using histograms. Histograms are computed in a manner analogous to that of Figure 10. The vertically-stratified earth model is perturbed with 10 heterogeneities with with (x_0, z_0) chosen randomly, y_0=1.1 (that is, on the fault plane), $(s_x, s_y, s_z) = (1, 1, 1$ km), and three different intensities of heterogeneity, $\sigma_v = 0.01$, 0.10 and 1.00 km/s. Bold: the traditional method, using absolute arrival time. Solid: double-difference method. The root-mean-square absolute traveltime error, ΔT, corresponding to each level of heterogeneity, σ_v, is given. Standard deviations, σ_x, of the traditional and double-difference estimates of horizontal position (in that order) are given for each plot. The traditional and double-difference methods yield similar errors.

a.

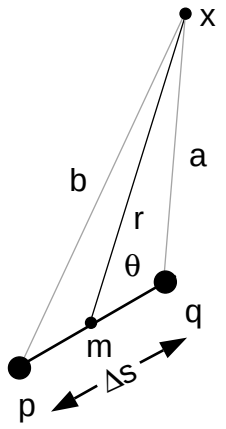
x
a
b
r
θ
q
m
Δs
p

b.

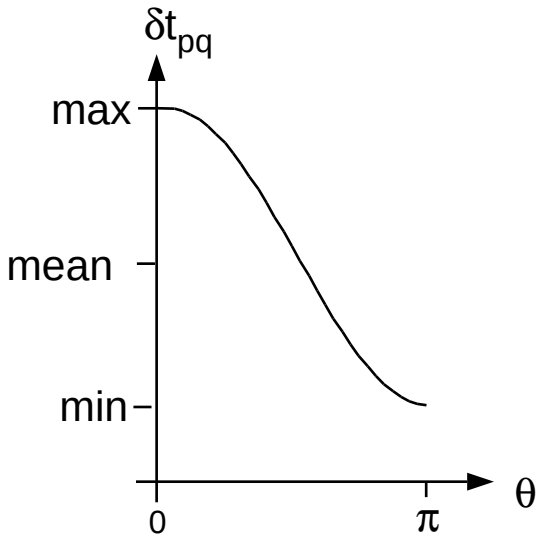
δt_pq
max
mean
min
0
π
θ

c.

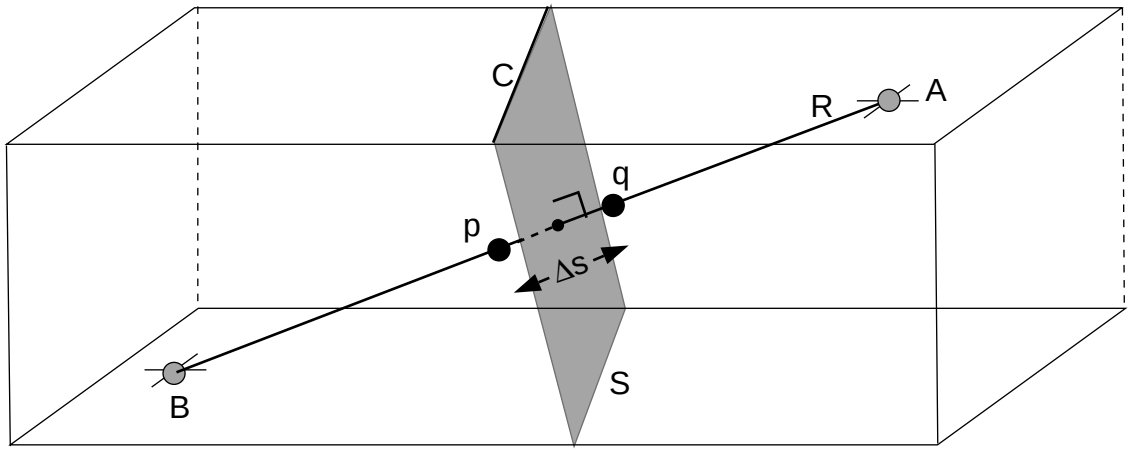
C
R
A
q
p
Δs
B
S

d.

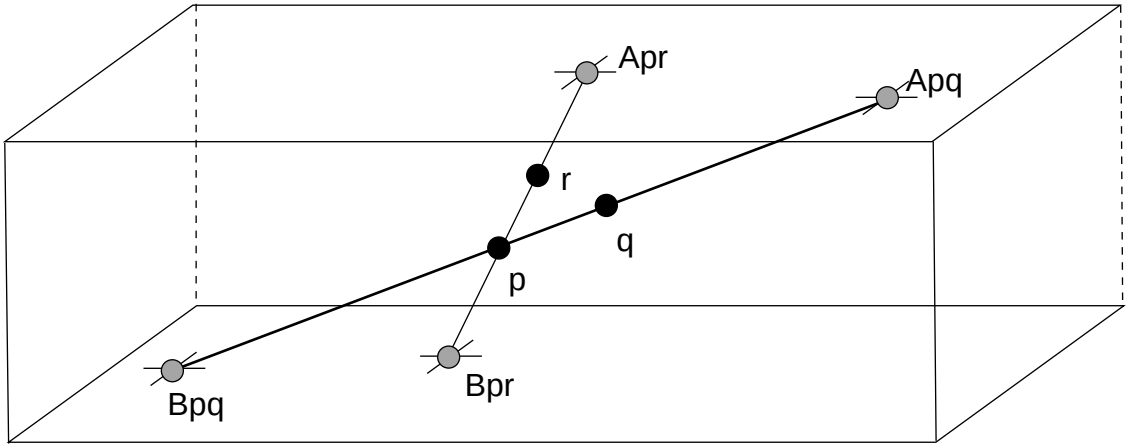
Apr
Apq
r
q
p
Bpq
Bpr

a.

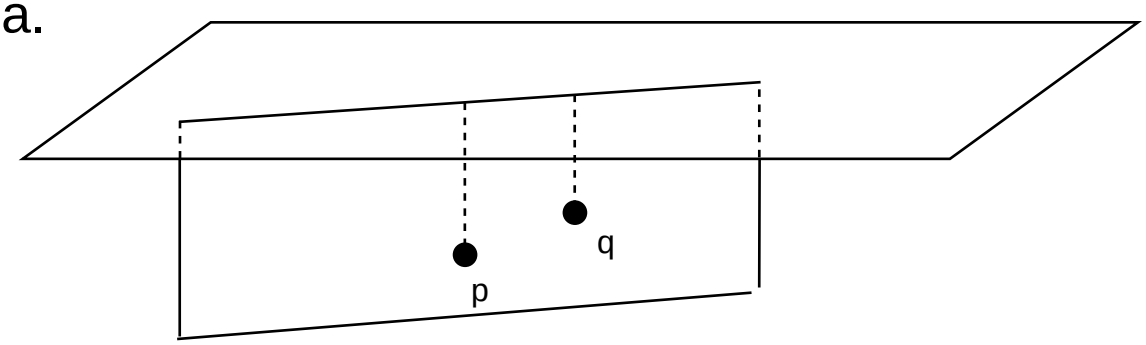

b.

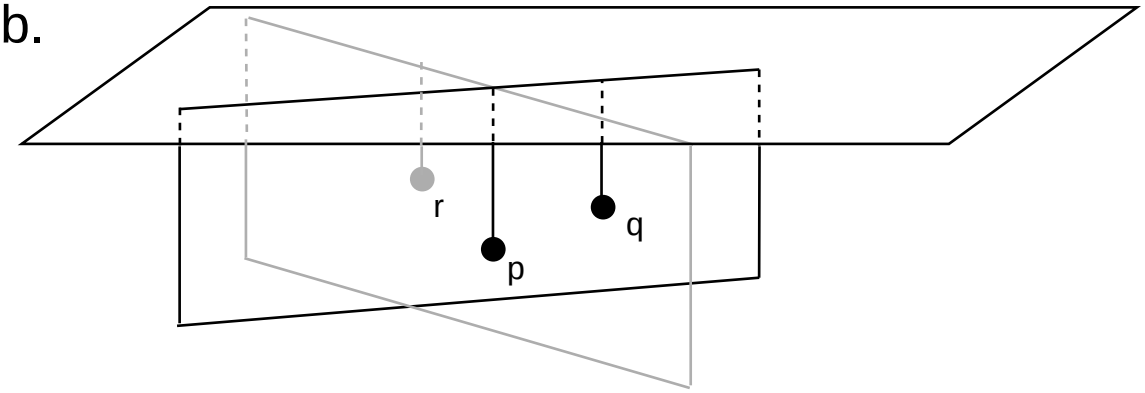

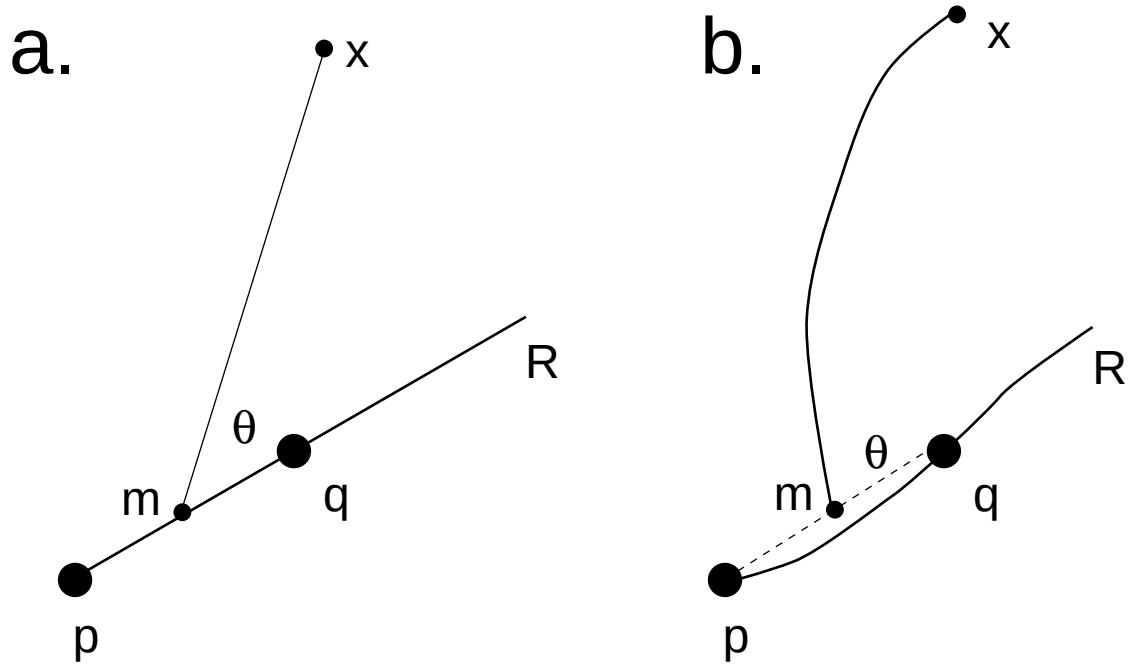
a.
x
R
θ
m
q
p
b.
x
R
θ
m
q
p

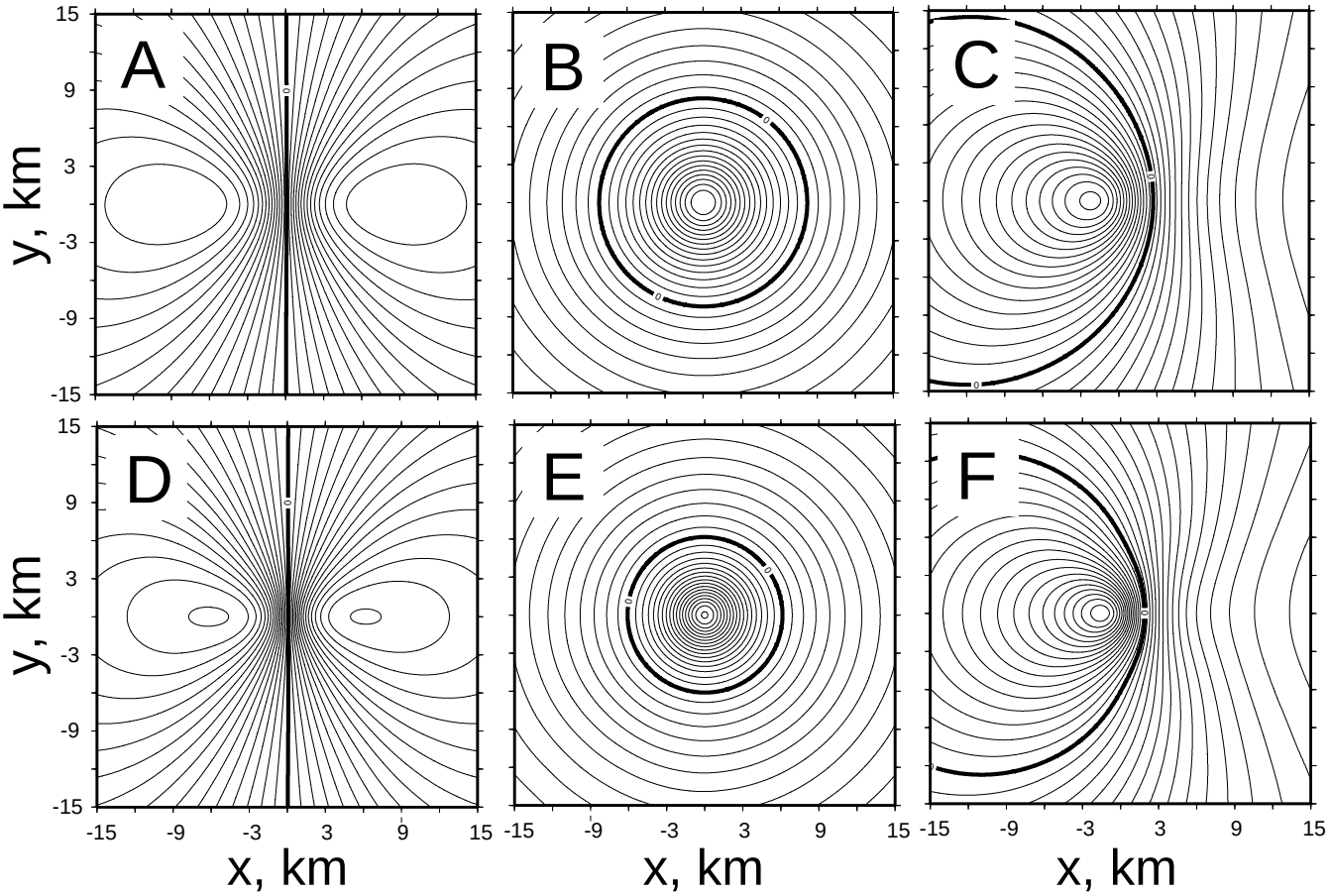
A
B
C
D
E
F
15
9
3
-3
-9
-15
y, km
-15
-9
-3
3
9
15
x, km

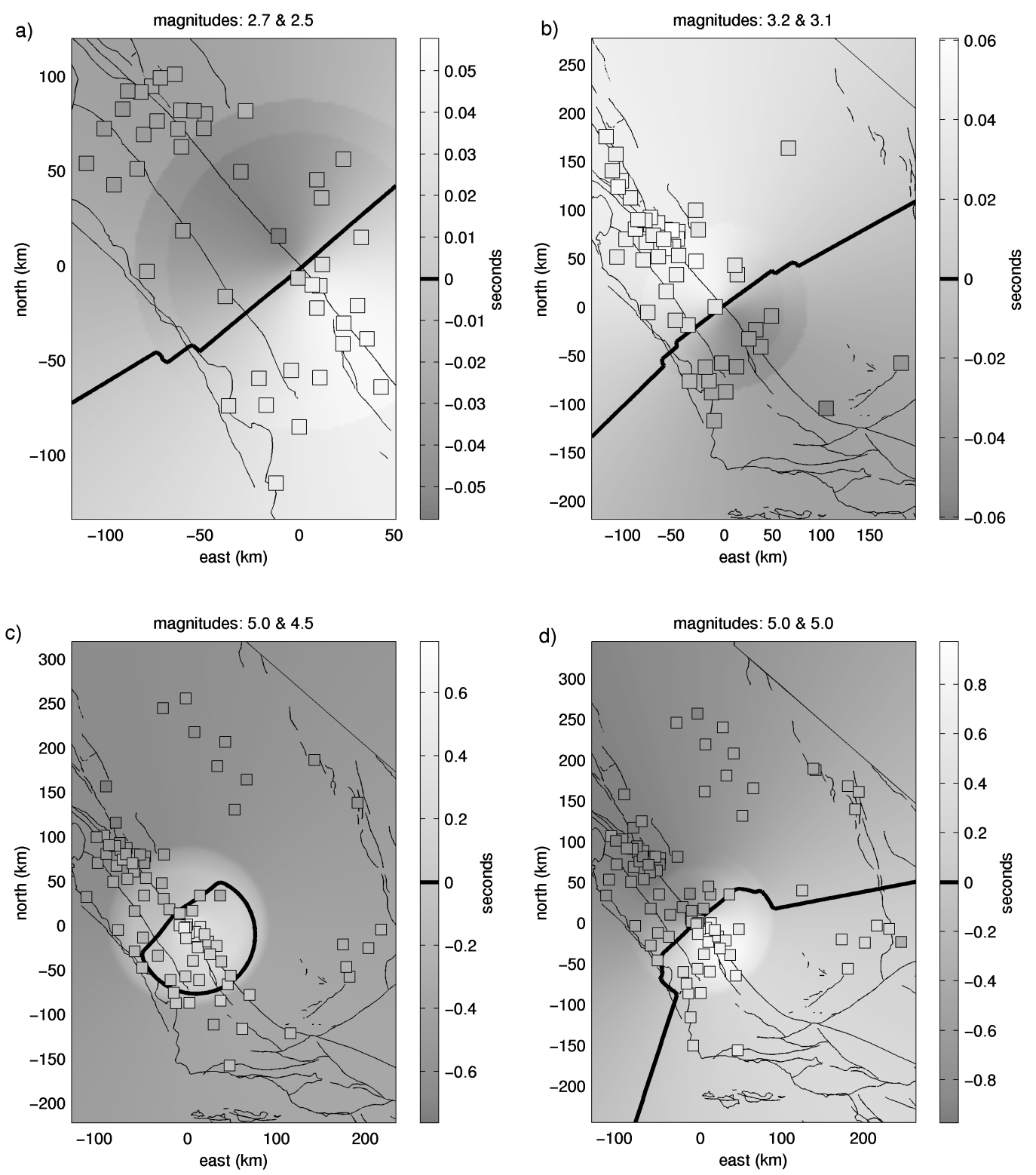
a)
magnitudes: 2.7 & 2.5
north (km)
east (km)
seconds
b)
magnitudes: 3.2 & 3.1
north (km)
east (km)
seconds
c)
magnitudes: 5.0 & 4.5
north (km)
east (km)
seconds
d)
magnitudes: 5.0 & 5.0
north (km)
east (km)
seconds

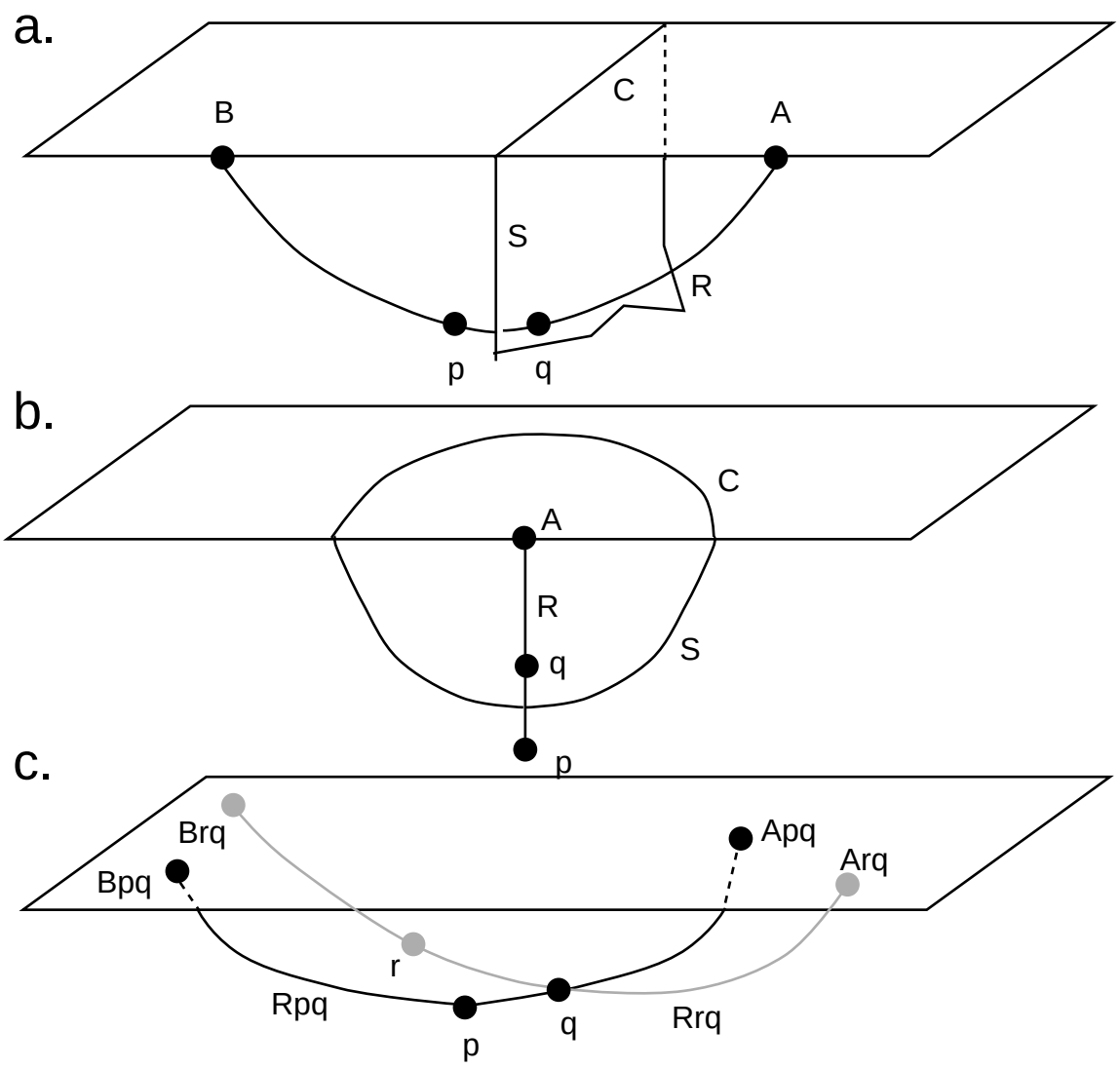
a.
B
C
A
S
R
p
q
b.
C
A
R
q
S
p
c.
Brq
Apq
Bpq
Arq
r
Rpq
q
Rrq
p

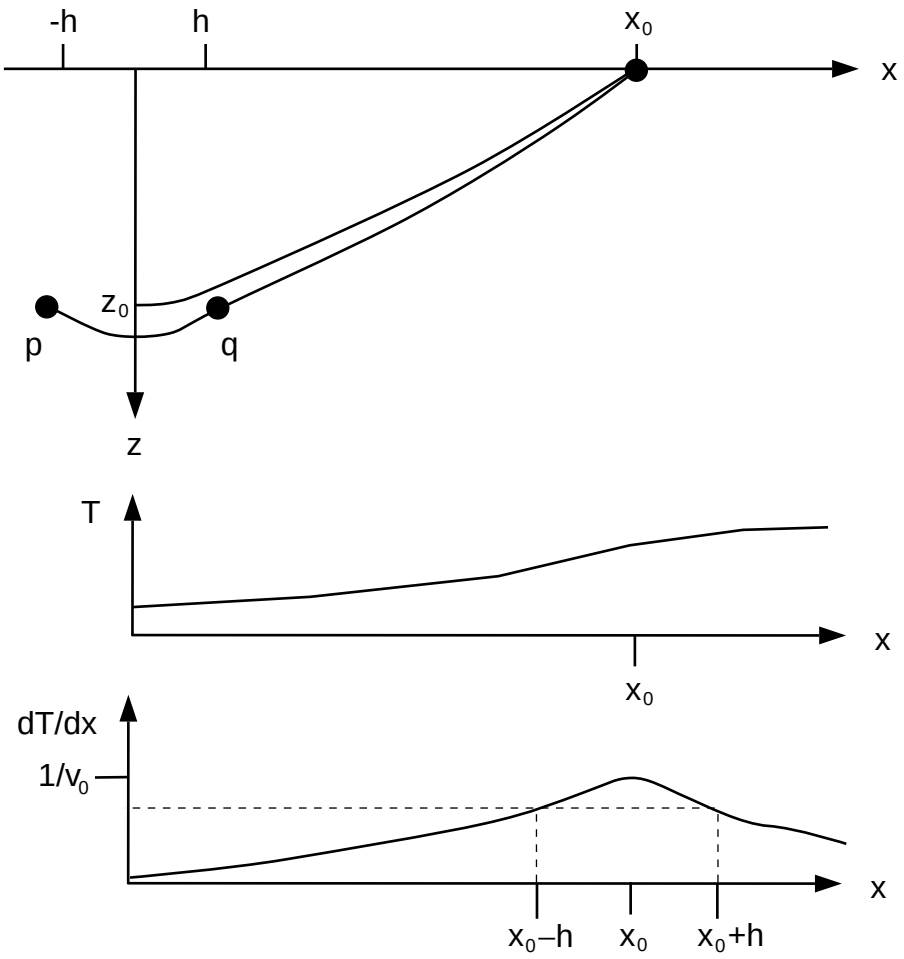
-h
h
x_0
x
z_0
p
q
z
T
x
x_0
dT/dx
$1/v_0$
x
x_0–h
x_0
x_0+h

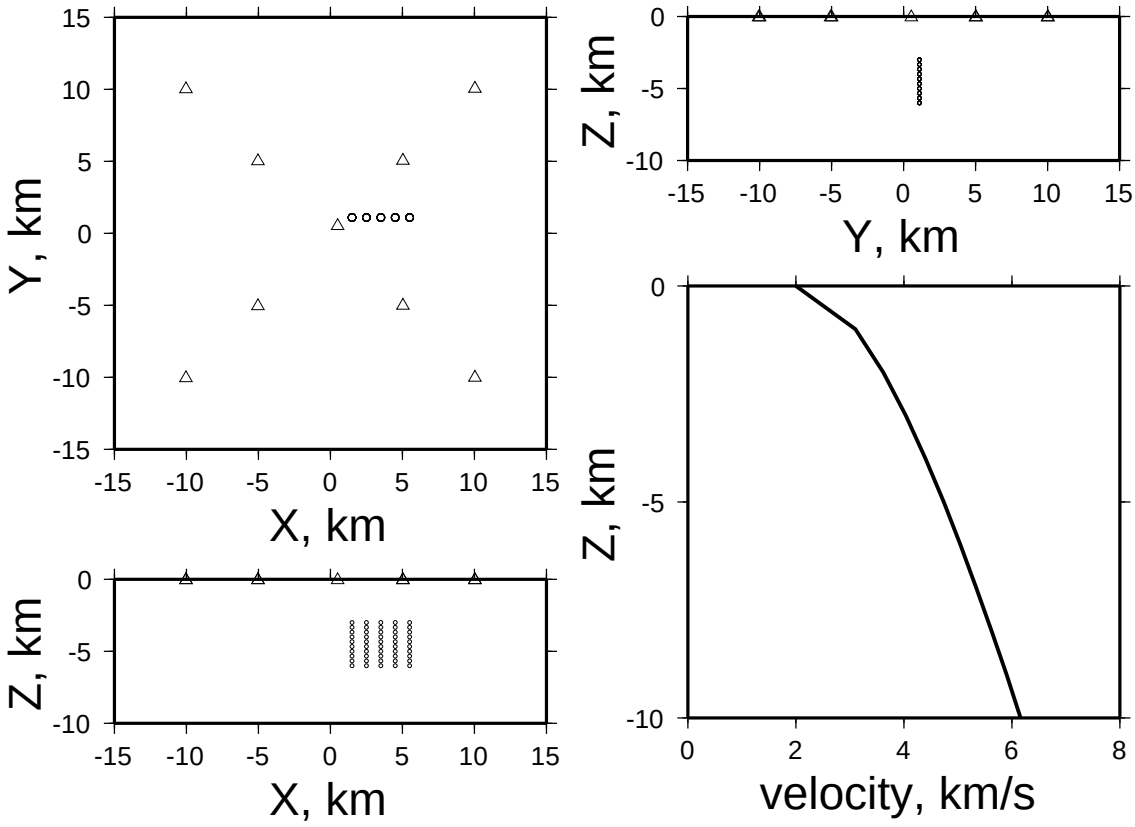
15
10
5
0
-5
-10
-15
Y, km
-15 -10 -5 0 5 10 15
X, km
0
-5
-10
Z, km
-15 -10 -5 0 5 10 15
X, km
0
-5
-10
Z, km
-15 -10 -5 0 5 10 15
Y, km
0
-5
-10
Z, km
0 2 4 6 8
velocity, km/s

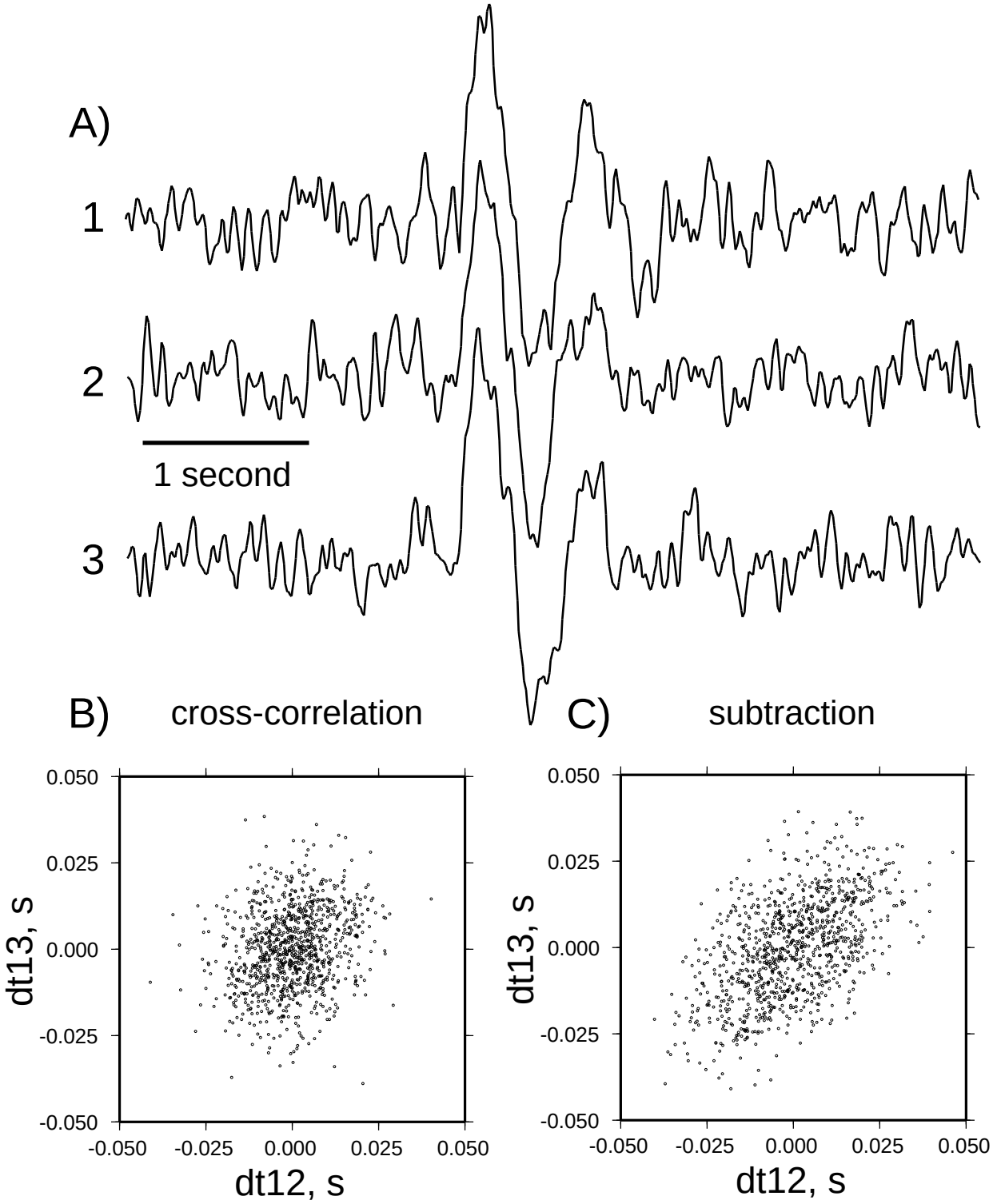
A)
1
2
1 second
3
B)
cross-correlation
C)
subtraction
0.050
0.025
0.000
-0.025
-0.050
dt13, s
dt12, s

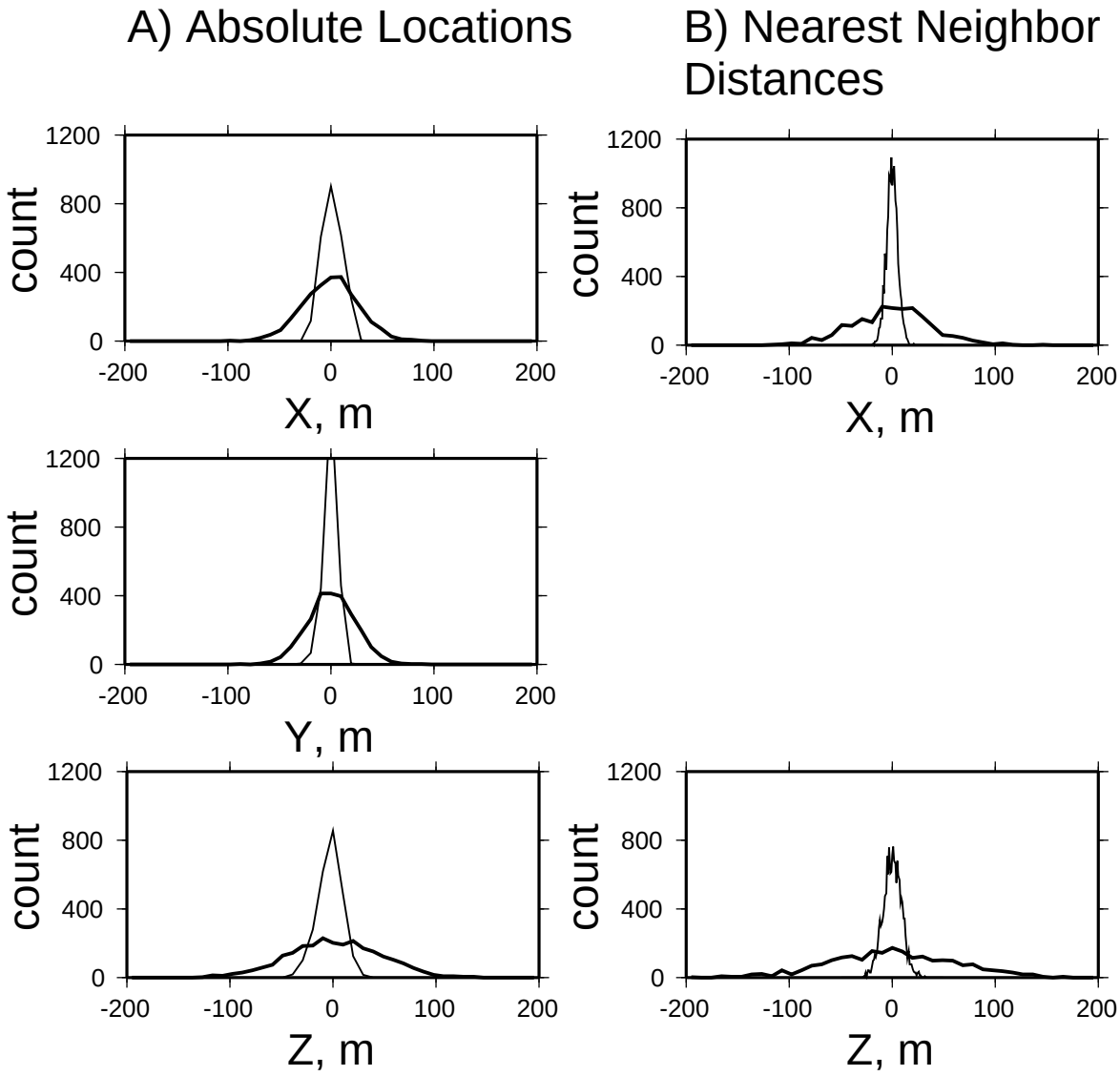
A) Absolute Locations
B) Nearest Neighbor Distances
count
1200
800
400
0
-200
-100
0
100
200
X, m
Y, m
Z, m

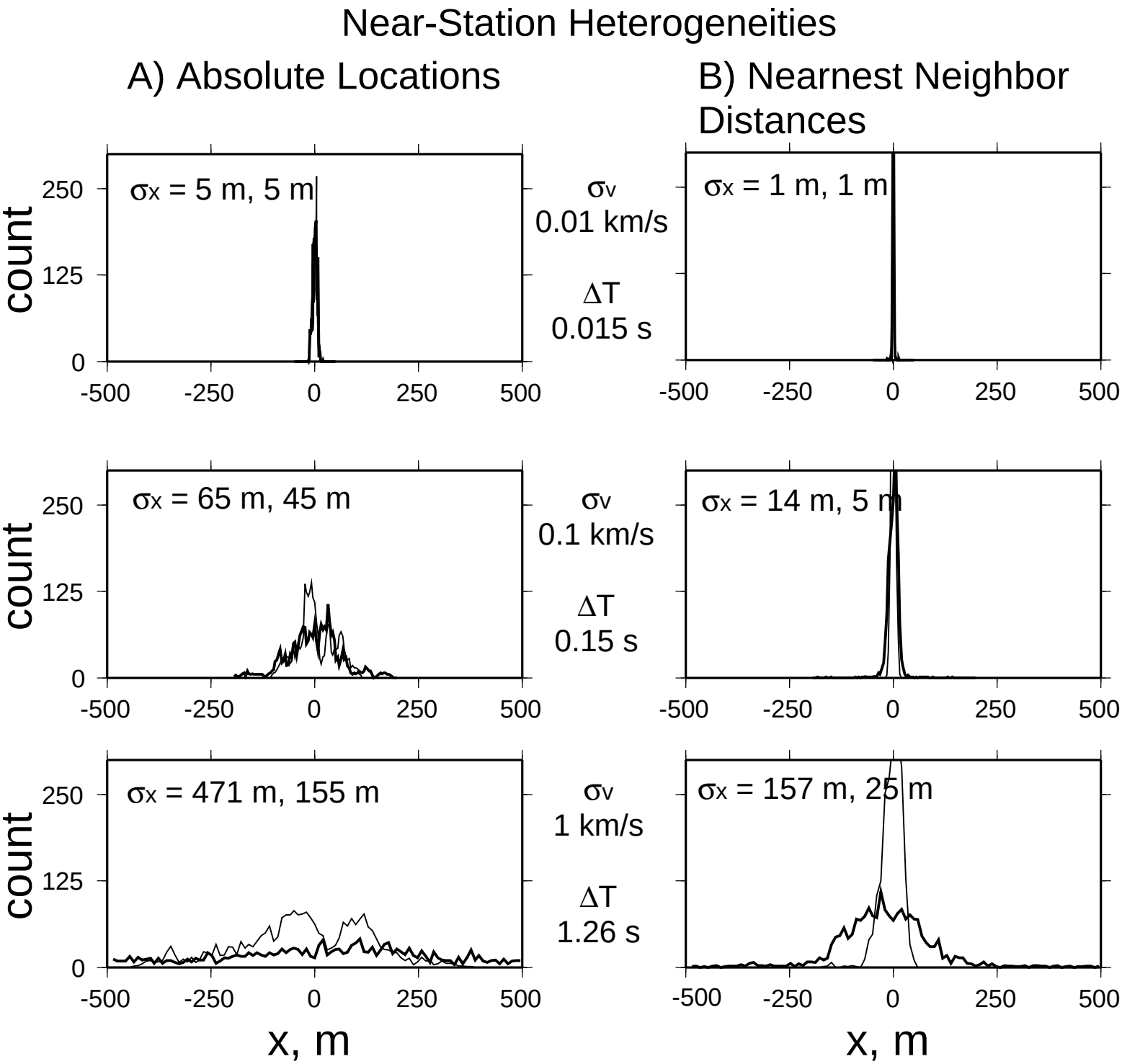
Near-Station Heterogeneities
A) Absolute Locations
B) Nearest Neighbor Distances
σx = 5 m, 5 m
σv
0.01 km/s
ΔT
0.015 s
σx = 1 m, 1 m
σx = 65 m, 45 m
σv
0.1 km/s
ΔT
0.15 s
σx = 14 m, 5 m
σx = 471 m, 155 m
σv
1 km/s
ΔT
1.26 s
σx = 157 m, 25 m
count
250
125
0
-500
-250
0
250
500
x, m

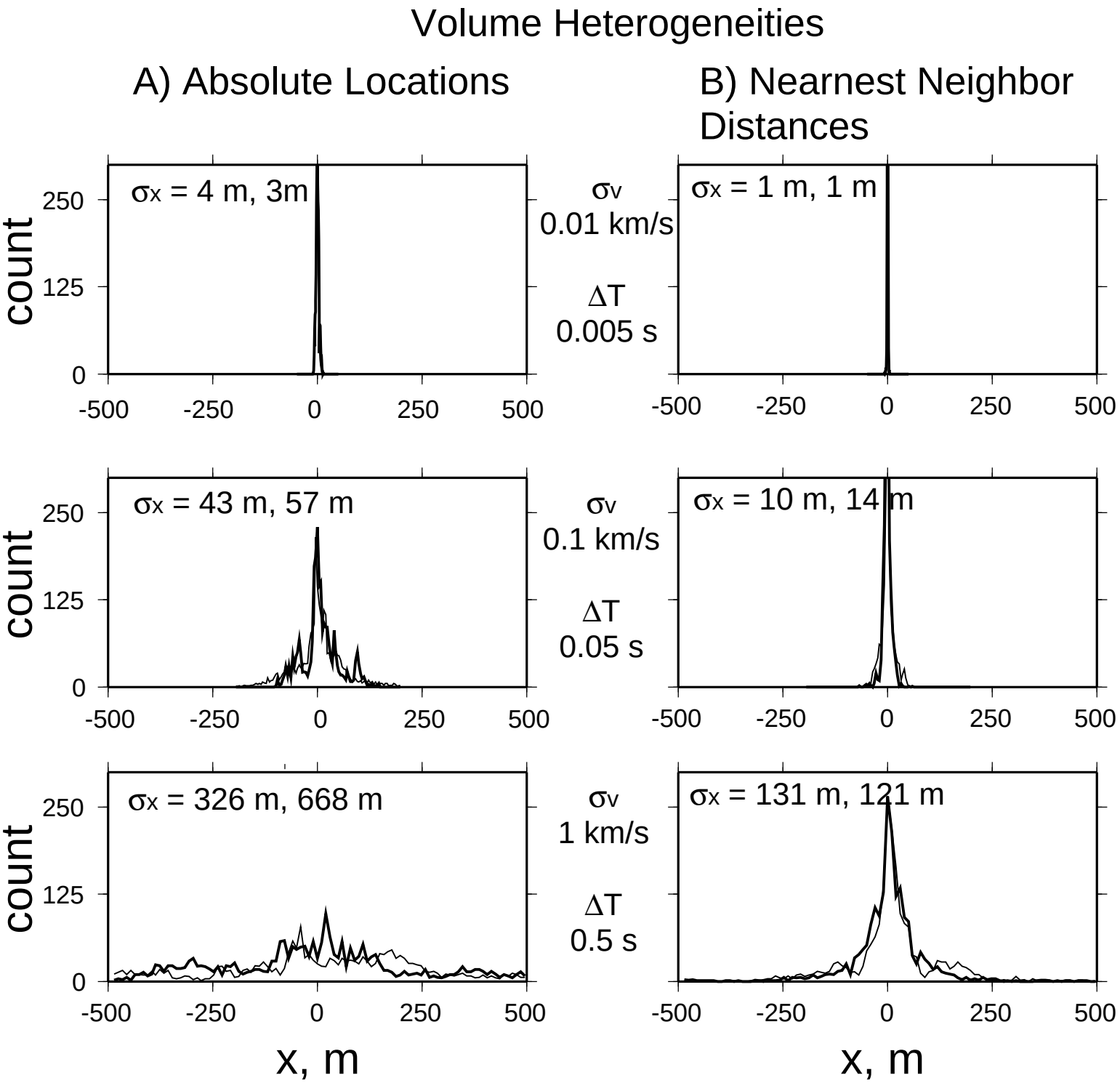
Volume Heterogeneities
A) Absolute Locations
B) Nearnest Neighbor Distances
σx = 4 m, 3m
σx = 1 m, 1 m
σv
0.01 km/s
ΔT
0.005 s
σx = 43 m, 57 m
σx = 10 m, 14 m
σv
0.1 km/s
ΔT
0.05 s
σx = 326 m, 668 m
σx = 131 m, 121 m
σv
1 km/s
ΔT
0.5 s
count
250
125
0
-500
-250
0
250
500
x, m

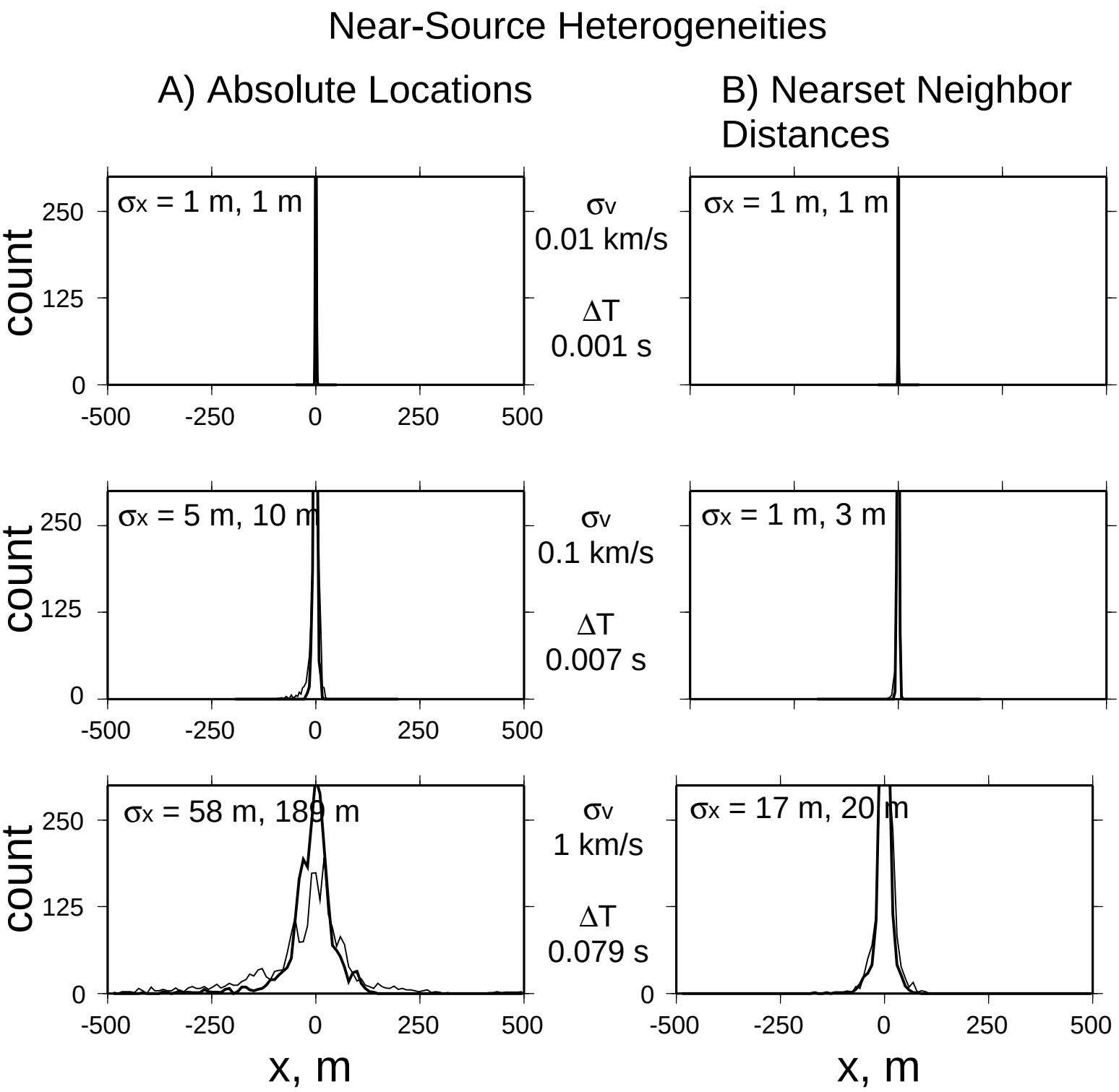
Near-Source Heterogeneities
A) Absolute Locations
B) Nearset Neighbor Distances
σx = 1 m, 1 m
σv
0.01 km/s
ΔT
0.001 s
σx = 1 m, 1 m
σx = 5 m, 10 m
σv
0.1 km/s
ΔT
0.007 s
σx = 1 m, 3 m
σx = 58 m, 189 m
σv
1 km/s
ΔT
0.079 s
σx = 17 m, 20 m
count
250
125
0
-500
-250
0
250
500
x, m